EFFECT OF ROTATION ON IGNITION THRESHOLDS OF STOICHIOMETRIC HYDROGEN-AIR MIXTURES

J. Melguizo-Gavilanes and J.E. Shepherd

Graduate Aerospace Laboratories, California Institute of Technology (GALCIT)
Pasadena, CA, USA, josuemg@caltech.edu

Abstract

Successful transition to a hydrogen economy calls for a deep understanding of the risks associated with its widespread use. Accidental ignition of hydrogen by hot surfaces is one of such risks. In the present study, we investigated the effect that rotation has on the reported ignition thresholds by numerically determining the minimum surface temperature required to ignite stoichiometric hydrogen-air using a hot horizontal cylinder rotating at various angular velocities, ω. Numerical experiments showed a weak but interesting dependence of the ignition thresholds on rotation: the ignition thresholds increased by 8 K, from 931 K to 939 K, with increasing angular velocity ($0 \leq \omega \leq 240$ rad/s). A further increase to ω = 480 rad/s resulted in a decrease in ignition surface temperature to 935 K. Detailed analysis of the flow patterns inside the vessel and in close proximity to the hot surface brought about by the combined effect of buoyancy and rotation, as well as of the distribution of the wall heat flux along the circumference of the cylinder, support our previous findings in which regions where temperature gradients are small were found to be prone to ignition.

1. INTRODUCTION

Improved scientific understanding and characterization of ignition is of prime importance to evaluating the risk of accidental fire and explosions in commercial aviation, nuclear power plants and the chemical process sector [1, 2]. While the study of the heat transfer characteristics from rotating bodies has been a topic of active study for decades due to its various engineering applications such as heat transfer from rotating machinery, spinning projectiles and others [3, 4, 5], interestingly, thermal ignition studies from rotating hot surfaces appear not to have been considered in previous theoretical, numerical or experimental work. Hot rotating shafts are ubiquitous in industrial settings and could pose an ignition hazard if they come in contact with combustible mixtures upon unintended or accidental releases. Careful study of the influence of rotation on thermal ignition thresholds is then an important aspect towards achieving a complete understanding of thermal ignition. The aim of the present study is to understand the influence of rotation on the ignition of stoichiometric hydrogen-air mixtures through two dimensional simulations using detailed chemistry where the ignition source is a hot rotating horizontal cylinder. Special attention is given to the dynamics of the ignition process as a function of angular velocity to unravel the key physical and chemical processes taking place near the ignition location.

2. COMPUTATIONAL METHODOLOGY

2.1. Governing equations, transport and chemical models

The motion, transport and chemical reaction in the gas surrounding the heated surface were modeled using the low Mach number, variable-density reactive Navier-Stokes equations with temperature-dependent transport properties [6]. Differential diffusion effects were taken into account using a constant but non-unity Lewis number for each species, Le_i, as proposed by [6]. The form that the heat and mass diffusion fluxes take when written as a function of Le_i can be found in [7] along with all the spatial and temporal discretization details, and models used to account for the functional temperature dependence of mixture viscosity, thermal conductivity and specific heat. Thermodiffusion (Soret effect) and radiation were neglected. The governing equations were solved using the Open source Field Operation And Manipulation (OpenFOAM) toolbox [8]. Our implementation of the code is well validated as it has been used successfully in various ignition studies comprising different geometries, modes of heat transfer (e.g. forced and natural convection), and ignition timescales [7, 9, 10, 11, 12]. The chemistry was modeled using Mével's mechanism for hydrogen oxidation which includes 9 species and 21 reactions [13, 14]. This mechanism has been extensively validated, and reproduces flame speeds and ignition delay times to a reasonable degree of accuracy over a wide range of concentrations.

2.2. Domain, initial and boundary conditions

The geometry simulated corresponded to a horizontal cylinder of radius $r = 5$ mm placed in the center of a combustion vessel of width 11.4 cm, depth 11.4 cm and height 15.5 cm. A detailed description of the vessel can be found in [9]. The mesh used was a two-dimensional (2D) planar cross section taken in the middle of the vessel including 109,000 cells in the computational domain. The cells were compressed near the wall of the heated surface, using a minimum cell size of approximately 40 μm to properly resolve the thermal and hydrodynamic boundary layers. The initial conditions were $\mathrm{p}_o = 101$ kPa, $\mathrm{T}_o = 300$ K, $\mathrm{U}_o = (0, 0)$ m/s, and mass fractions $\mathrm{Y}_{\mathrm{H}_2} = 0.0283$, $\mathrm{Y}_{\mathrm{O}_2} = 0.2264$, $\mathrm{Y}_{\mathrm{N}_2} = 0.7453$, corresponding to a stoichiometric hydrogen-air mixture. On the heated surface: for temperature, a time dependent boundary condition given by $\mathrm{T}_{\mathrm{surf}}$ (t) = 300 + α t was imposed with a heating rate of $\alpha = 220$ K/s; for velocity, a rotating boundary condition was used with the axis of rotation located at the center of the cylinder, and positive (counterclockwise) constant angular velocities, ω, of 60, 120, 240 and 480 rad/s. Additionally, a stationary case ($\omega = 0$ rad/s) was run to use as a reference. A rationale for the choice of angular velocities is given in the next section.

3. RESULTS AND DISCUSSION

Numerical fields of temperature, magnitude of velocity and velocity vectors, and mass fraction of HO_2 (important intermediate species) during ignition and early stages of flame propagation are shown in this section for $\omega = 0$, 120, 240 and 480 rad/s to illustrate the differences in the ignition evolution. The time to ignition was found by monitoring the gas temperature, T, until its maximum in the computational domain reached 150 K beyond the heated surface temperature, $\mathrm{T}_{\mathrm{surf}}$ (t). Note that the stiff nature of hydrogen chemistry makes the ignition time, hence $\mathrm{T}_{\mathrm{surf}}$, insensitive to the choice of threshold temperature.

3.1. Flow field and ignition evolution

To properly understand the effect that rotation has on ignition thresholds is important to first study the flow patterns induced inside the vessel and in close proximity to the hot surface when a rotating boundary condition is imposed, and compare them against a reference stationary case (ω = 0 rad/s).

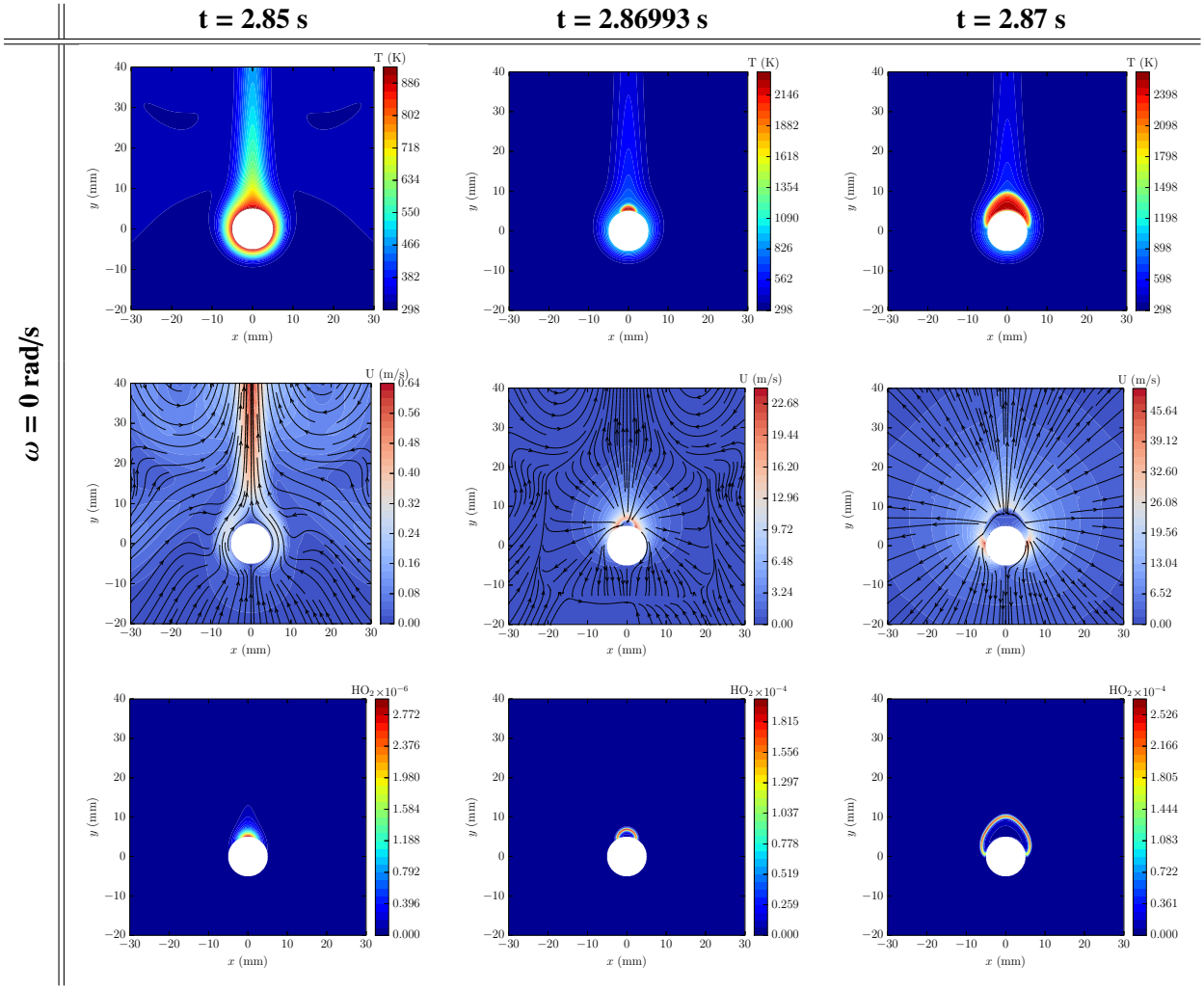

Figure 1: ω = 0 rad/s (reference case) - temperature, magnitude of velocity and HO_2 mass fraction fields during ignition and early stages of flame propagation.

Figure 1 shows the ignition evolution for ω = 0 rad/s. Shortly before ignition, t = 2.875 s, the buoyancy flow induced by the heating of the cylinder results in the thermal boundary layer and thermal plume that can be clearly observed in the temperature field. The thermal boundary layer appears to have a constant thickness on both sides of the cylinder, and grows in the direction of the flow. The velocity field shows the entrainment of cold gas starting at the front stagnation point of the cylinder, (x,y) = (0,–5) mm, which travels along its circumference to then continue its upward journey within the thermal plume. The maximum velocity within the thermal plume is 0.6 m/s approximately. The HO_2 mass fraction field reveals that chemical activity is confined to the top of the cylinder i.e. back stagnation point (0,5) mm, where the thermal boundary layer merges with the thermal plume. Twenty milliseconds later, at t = 2.86993 s, an ignition kernel forms at the top of the cylinder and subsequently propagates as a laminar flame preferentially consuming the hot reactants present in the thermal plume and boundary layer. The surface temperature at ignition for this case was $T_{surf} \sim 931$ K. The angular location where ignition takes

place was measured taking the front stagnation point as a reference, $\theta = 0$, and normalized by π (180°). Following the standard convention (right hand rule), angles measured in a counterclockwise direction from the negative y-axis are positive (right side of the cylinder), and negative otherwise (left side of the cylinder). The ignition location for the reference case was $\theta = \pm\ 180°$ ($\theta/\pi = \pm\ 1$).

The maximum plume velocity before ignition for the stationary case ($U_{p,\max@ign}$) was used to select the rotational speeds, or angular velocities, ω, in this study. Specifically, we chose cases where the tangential velocity, $U_t = r\omega$, on the cylinder surface were $0.5U_{p,\max@ign}$, $U_{p,\max@ign}$, $2U_{p,\max@ign}$, and $4U_{p,\max@ign}$ to induce an appreciable change in the resulting flow field. Consequently, the corresponding angular velocities were 60, 120, 240 and 480 rad/s, respectively. While we report ignition thresholds and locations for all values of ω considered, we only present details of the flow field for 120, 240 and 480 rad/s.

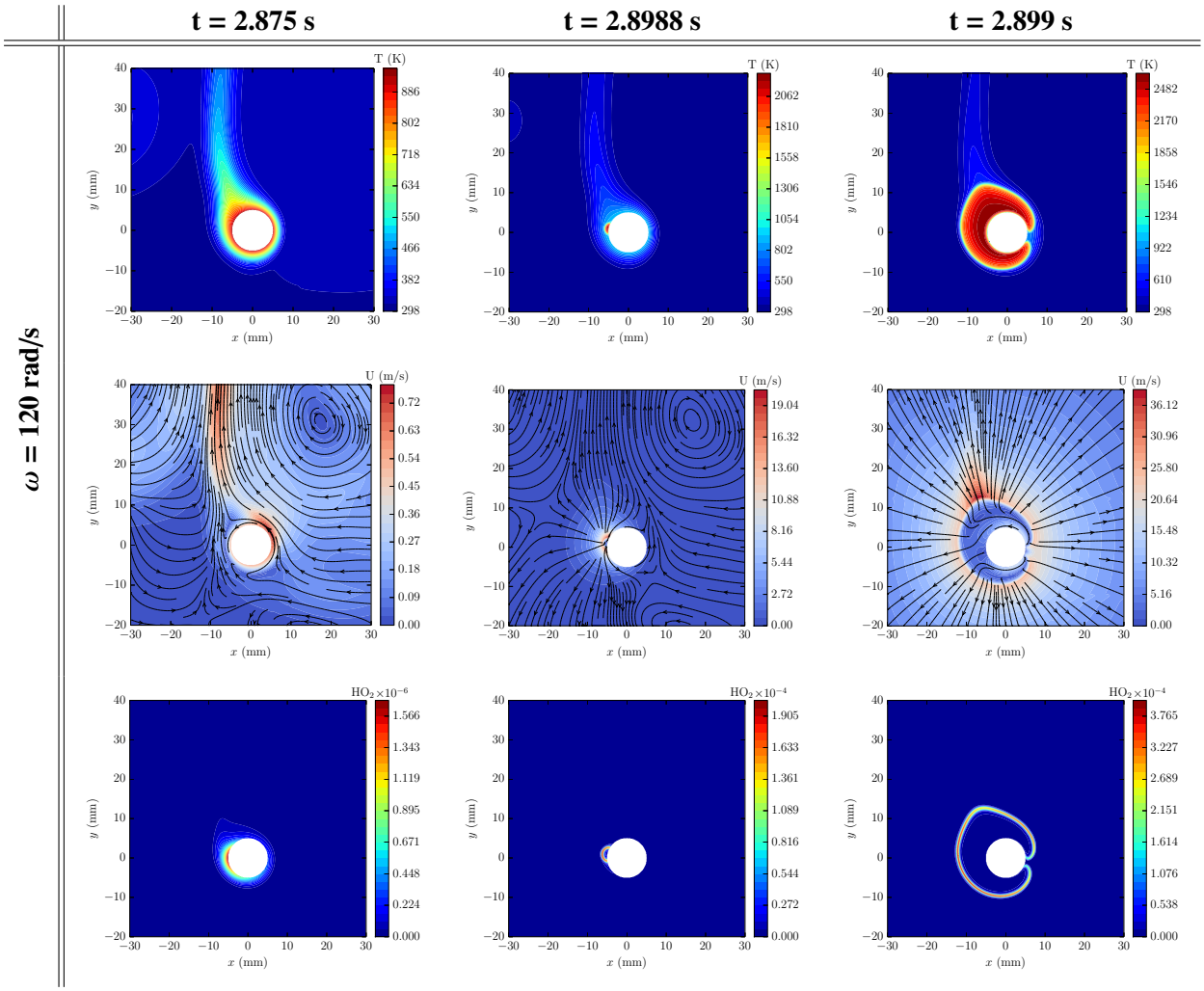

Figure 2: ω = 120 rad/s - temperature, magnitude of velocity and HO_2 mass fraction fields during ignition and early stages of flame propagation.

Figure 2 shows the case in which the tangential velocity, $U_t = r\omega = 0.6$ m/s ($\omega = 120$ rad/s), is of the same order of the maximum plume velocity before ignition in the stationary case ($U_t/U_{p,\max@ign} \sim 1$). In contrast with the reference case, the thermal boundary layer is no longer of the same thickness on both sides of the cylinder. This is a direct consequence of the rotational speed imposed at the surface and the buoyancy flow induced by the heating of the cylinder. For $x > 0$ (right side of the cylinder), the motion

induced by the rotation and buoyancy have the same direction. This results in higher velocities on this side of the cylinder and consequently a thinner thermal boundary layer (see Temperature and Velocity fields at t = 2.875 s). For $x < 0$ (left side of the cylinder) however, the motion induced by the rotation of the cylinder and buoyancy have opposite directions. This results in low velocities in this region and a thicker thermal boundary layer. Note that the velocity vectors reveal a boundary layer separation-like pattern around (–5,4) mm which brings the flow almost to rest enhancing chemical activity in this area (see HO_2 mass fraction field). This is in line with previous observations [7, 15] where the dynamics of ignition by moving spheres and stationary hot surfaces was analyzed. The interaction of buoyancy and rotation offsets the thermal plume from the center of the cylinder, and moves the ignition location from $\theta = \pm 180°$ to $\theta = -134°$ ($\theta/\pi = -0.75$). The surface temperature at ignition was $T_{surf} \sim 938$ K, approximately 7 K higher than the reference case. The different shape that the flame takes compared to the reference case is a consequence of the non-uniform temperature field that results from the heating and rotation of the cylinder, and associated higher burning speeds in the hot reactants present in the thermal plume and boundary layer.

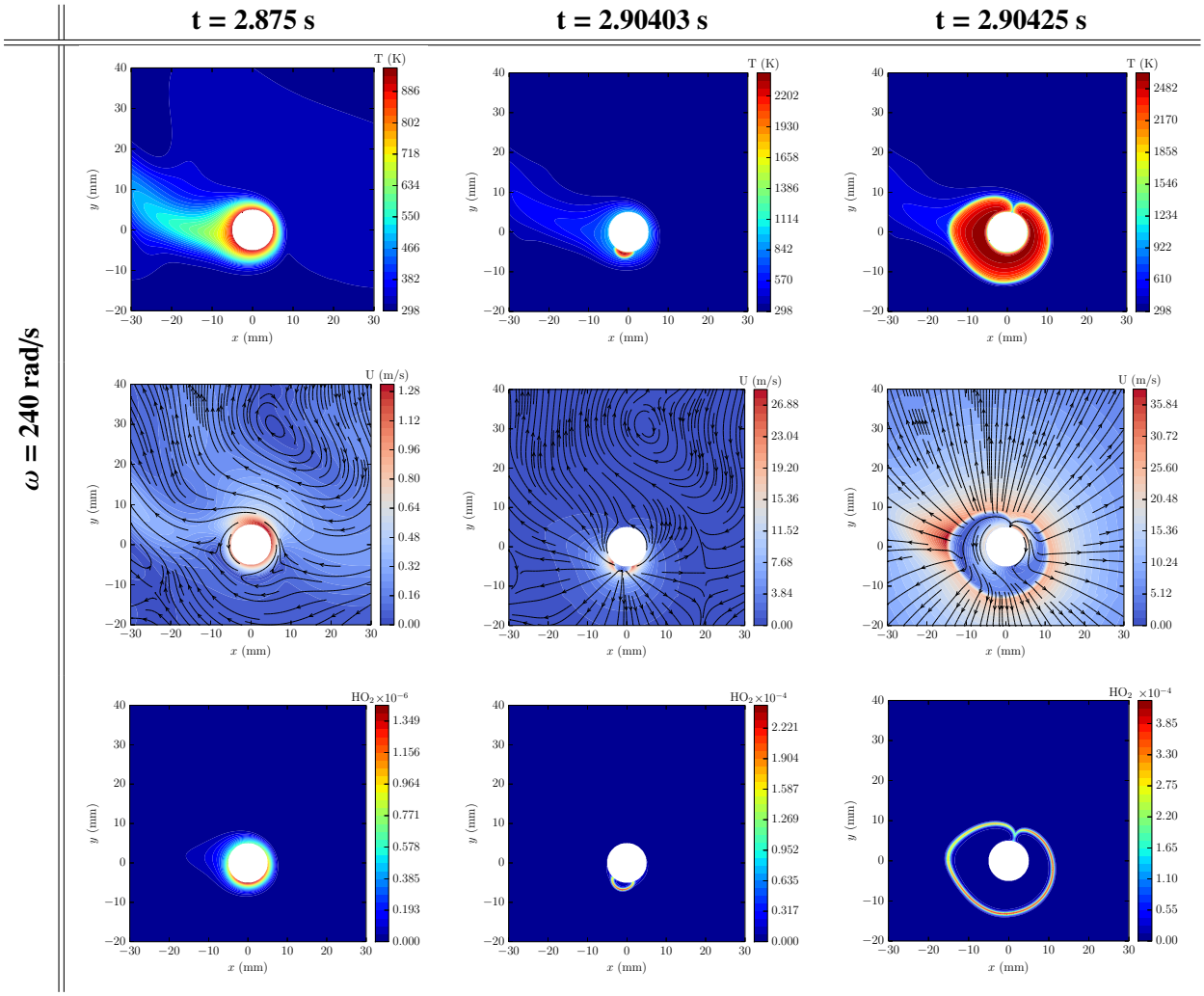

Figure 3: ω = 240 rad/s - temperature, magnitude of velocity and HO_2 mass fraction fields during ignition and early stages of flame propagation.

A further increase in the angular velocity to ω = 240 rad/s ($U_t/U_{p,max@ign} \sim 2$) yields a more noticeable change in the flow field than in the previous two cases. The higher rotational speed delays the onset of buoyancy and it only becomes active once heat diffuses significantly far away from the cylinder surface

($x < 0$). This lighter gas then tends to rise, and creates the distorted, almost horizontal plume seen in the temperature field of Fig. 3 at t = 2.875 s. Similarly to what was described above, a boundary layer separation-like pattern is created, but in this case closer to the front stagnation point (see Velocity field). Shortly after, ignition occurs around $\theta = -23°$ ($\theta/\pi = -0.13$) at a surface temperature, T_{surf}, of 939 K. Note that, in contrast with the previous cases, chemical activity does not appear to be as localized since it covers predominantly the bottom half of the sphere ($y < 0$). See HO_2 mass fraction field.

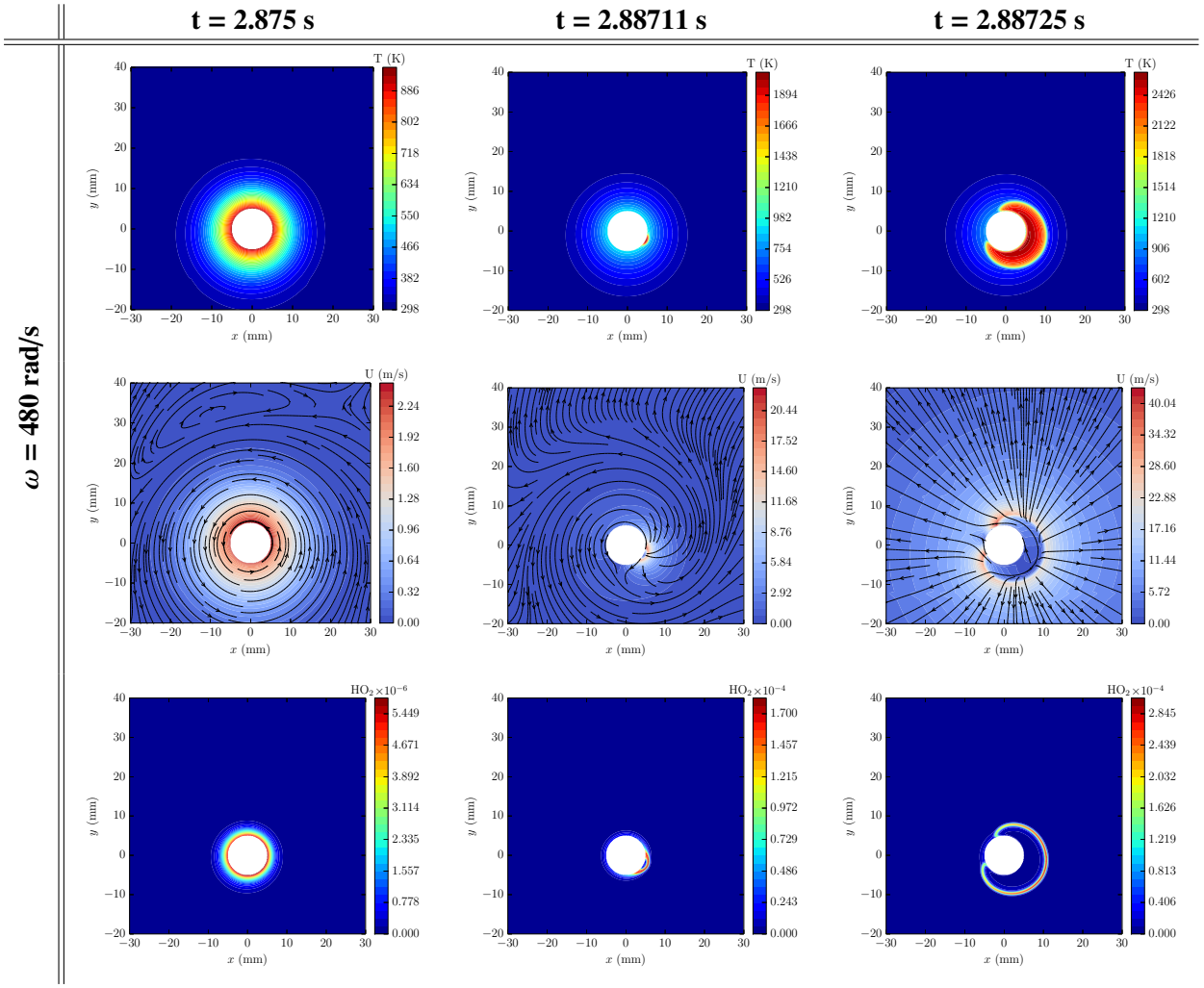

Figure 4: ω = 480 rad/s - temperature, magnitude of velocity and HO_2 mass fraction fields during ignition and early stages of flame propagation.

For a U_t to $U_{p,max@ign}$ ratio of 4 (ω = 480 rad/s), the effect of rotation fully overtakes buoyancy. The nature of the flow field is completely different to the previous cases. The streamlines show mainly rotational motion up to two diameters away from the surface of the cylinder. The temperature field returns to a more symmetric configuration with essentially equal thermal boundary layers on both sides of the cylinder. No thermal plume is present in this case. The production of HO_2 is evenly distributed over the circumference of the cylinder, and 4 and 3.5 times higher in value than for 240 rad/s and 120 rad/s at the same surface temperature, $T_{surf} \sim 932$ K (t = 2.875 s). This stronger chemical activity finally results in a slightly lower ignition threshold than in the previous two cases, namely ~ 935 K. Although visually, the distribution of HO_2 seems uniform, closer inspection of Fig. 4 shows slightly higher values for $x > 0$. Due to the high sensitivity of stoichiometric hydrogen-air mixtures in this temperature range, any non-uniformity or temperature perturbation will trigger an ignition. Specifically

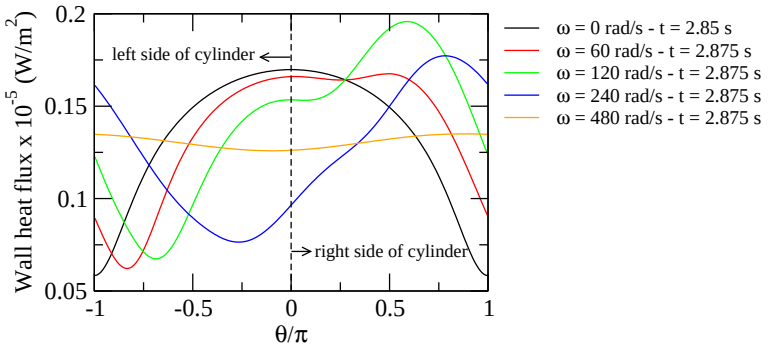

Figure 5: Wall heat flux along heated surface for all angular velocities considered - black (ω = 0 rad/s - reference case); red (ω = 60 rad/s); green (ω = 120 rad/s); blue (ω = 240 rad/s); orange (ω = 480 rad/s);

for this case, ignition occurred on the right hand side of the cylinder around $\theta = 52°$ ($\theta/\pi = 0.29$).

A more precise way of capturing the, in some cases, subtle differences in thermal boundary layer thickness and associated temperature gradients is by plotting the wall heat flux along the circumference of the cylinder across the angular velocity range considered (see Fig. 5). This plot gives a good indication of regions that are more likely to ignite because where the temperature gradients are shallow, or alternatively where the wall heat flux is low, higher temperatures are reached further away from the hot surface, minimizing heat losses, and resulting in higher reaction rates and more heat deposition in the gas [10]. The plot shows two different/asymmetric branches for all angular velocities, except for the stationary case (ω = 0 rad/s). This is because for the stationary case, the heat transfer is the same on both sides of the cylinder (symmetric about the vertical axis). See black line in Fig. 5. For 60, 120, 240 and 480 rad/s negative values of θ/π show the wall heat flux for left side of the cylinder ($x < 0$) and positive values of θ/π for the right side ($x > 0$). The profiles in Fig.5 are taken shortly before ignition for all angular velocities, and clearly show the effect that rotation has on the heat transfer characteristics of the cylinder. Moderate rotational speeds (60 – 120 rad/s) result in large differences in the thermal boundary layer thickness between the left and right side of the cylinder. This is a direct consequence of having comparable buoyancy induced and tangential velocities as was explained in subsection 3.1. Higher rotational speeds, ω = 480 rad/s, result in thicker thermal boundary layers and a wall heat flux that is essentially constant along the circumference of the cylinder only displaying a slight increase towards the back stagnation point ($\theta/\pi = \pm 1$).

3.2. Predicted ignition thresholds

Figure 6 summarizes the results described above in terms of surface temperature at ignition, T_{surf}, and ignition location, θ/π. There seems to be a weak but interesting dependence of the ignition thresholds on rotation. The ignition thresholds increase by 8 K, from 931 K to 939 K, with increasing angular velocity ($0 \leq \omega \leq 240$ rad/s). Interestingly, a further increase to 480 rad/s results in a decrease in ignition surface temperature to 935 K. Regarding ignition location, the point of ignition is brought from the back stagnation point ($\theta/\pi = \pm 1$) towards the front ($\theta/\pi = 0$) with increasing angular velocity ($0 \leq \omega \leq 240$ rad/s), and it crosses over the front of the cylinder to the right side ($x > 0$) for ω = 480 rad/s.

While for all practical purposes a difference of less than 10 K in ignition threshold would mean that

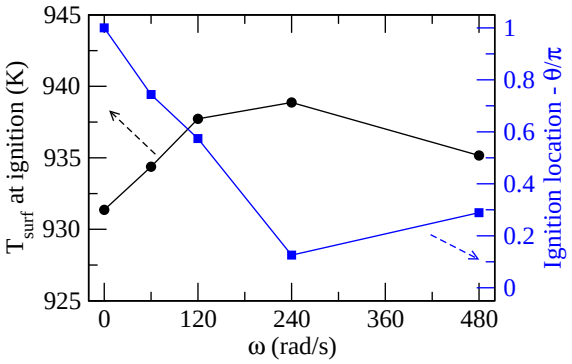

Figure 6: Surface temperature at ignition T_{surf} (black line) and ignition location (blue line) as a function of angular velocity.

the threshold for stoichiometric hydrogen-air remains essentially unchanged as a function of angular velocity, it is important to note that this outcome is only applicable to the mixture at hand, and that hydrocarbons with strong negative temperature coefficient (NTC) regions (faster ignition delay time at lower temperatures) could exhibit a stronger dependence. Additionally, imposing significantly faster rotational speeds could continue to yield a decreasing trend due to the changes induced in the flow field and resulting thicker thermal boundary layers, but it is unlikely that for stoichiometric hydrogen-air mixtures the thresholds will fall below 930 K. This is due to the strong change in activation energy characteristic of hydrogen chemistry in this temperature range which results in ignition delay times that are orders of magnitude shorter above 930 K.

4. CONCLUSION

The ignition of stoichiometric hydrogen-air mixtures by a horizontal cylinder rotating at various angular velocities was numerically investigated. To the authors knowledge this is the first time a 2D numerical simulation with detail chemistry is performed to investigate the effect of rotation on the reported ignition thresholds. Temperature, velocity and HO_2 mass fraction fields were used to explain the ignition evolution and quantify the effect of rotation on the minimum surface temperature required to ignite the mixture. Results showed that the ignition thresholds for the mixture considered are essentially unaffected by imposing a rotating boundary condition at the surface of the cylinder, showing only a variation of 8 K over the range of angular velocities studied. Ratios of tangential velocity at the surface of the cylinder to the maximum plume velocity induced by the heating of the cylinder in the stationary/reference case ($U_t/U_{p,\max@ign}$) between 0.5 and 2, yielded an increase in ignition threshold from 931 K to 939, respectively. Higher ratios, namely $U_t/U_{p,\max@ign} = 4$, resulted in a slight decrease in threshold to 935 K. The location of ignition along the surface of the cylinder showed a stronger variation as a function of angular velocity. Specifically, the ignition location moved from the back stagnation point of the cylinder towards the front (and beyond) with increasing angular velocity. Analysis of the wall heat flux along the surface of the cylinder revealed the regions that are more likely to ignite: those with shallow temperature gradients (low wall heat flux) as higher temperatures are reached further away from the cylinder, minimizing heat losses, and resulting in higher reaction rates and more heat deposition in the gas. This outcome highlights the importance of capturing properly the interaction of the hot surface with the buoyancy flow induced by the heating of the gas and imposed boundary conditions (rotation) if quantitative numeri-

cal predictions of ignition thresholds are sought. It is precisely this interaction that results in regions where the thermal boundary layer is thicker favoring the establishment of the critical conditions for ignition to occur. Future work will include expanding the range of angular velocities considered, detailed analysis of temperature, velocity and species profiles at the ignition location, as well as analysis of the competition of convective, diffusive and chemical reaction terms within the thermal boundary layer.

ACKNOWLEDGMENTS

This work was carried out in the Explosion Dynamics Laboratory of the California Institute of Technology, J. Melguizo-Gavilanes was supported by The Boeing Company through a Strategic Research and Development Relationship Agreement CT-BA-GTA-1. This work used the Extreme Science and Engineering Discovery Environment (XSEDE) which is supported by National Science Foundation grant number ACI-1548562.

REFERENCES

1. B. Stack, A. Sepeda, and M. Moosemiller. Guidelines for determining the probability of ignition of a released flammable mass. *Process Safety Progress*, 33(1):19–25, 2014.
2. V. Babrauskas. *Ignition handbook*, volume 98027. Fire Science Publishers, Issaquah, WA, 2003.
3. H.M. Badr and S.C.R. Dennis. Laminar forced convection from a rotating cylinder. *International journal of heat and mass transfer*, 28(1):253–264, 1985.
4. R.I. Elghnam. Experimental and numerical investigation of heat transfer from a heated horizontal cylinder rotating in still air around its axis. *Ain Shams Engineering Journal*, 5(1):177–185, 2014.
5. H. Ma, Z. Ding, Y. Cao, X. Lv, W. Lu, X. Shen, and L. Yin. Characteristics of the heat transfer from a horizontal rotating cylinder surface. *Experimental Thermal and Fluid Science*, 66:235–242, 2015.
6. T. Poinsot and D. Veynante. *Theoretical and Numerical Combustion*. Edwards, 2005.
7. J. Melguizo-Gavilanes, L.R. Boeck, R. Mével, and J.E. Shepherd. Hot surface ignition of stoichiometric hydrogen-air mixtures. *International Journal of Hydrogen Energy*, 2016.
8. H. G. Weller, G. Tabor, H. Jasak, and C. Fureby. A tensorial approach to computational continuum mechanics using object-oriented techniques. *Computers in Physics*, 12(6):620–631, 1998.
9. J. Melguizo-Gavilanes, A. Nové-Josserand, S Coronel, R Mével, and J.E. Shepherd. Hot surface ignition of n-hexane mixtures using simplified kinetics. *Combustion Science and Technology*, 2016.
10. J. Melguizo-Gavilanes, R. Mével, S. Coronel, and J.E. Shepherd. Effects of differential diffusion on ignition of stoichiometric hydrogen-air by moving hot spheres. *Proceedings of the Combustion Institute*, 2016.
11. R. Mével, U. Niedzielska, J. Melguizo-Gavilanes, S. Coronel, and J.E. Shepherd. Chemical kinetics of ignition of *n*-hexane by a moving hot sphere. *Combustion Science and Technology*, 2016.
12. J. Melguizo-Gavilanes, P.A. Boettcher, A. Gagliardi, V.L. Thomas, and R. Mével. Two-dimensional numerical simulation of the transition between slow reaction and ignition. *Proceedings of the 9th Joint US Sections Meeting of the Combustion Institute, 2015*, 2015.
13. R. Mével, S. Javoy, F. Lafosse, N. Chaumeix, G. Dupré, and C. E. Paillard. Hydrogen-nitrous oxide delay time: shock tube experimental study and kinetic modelling. *Proceedings of The Combustion Institute*, 32:359–366, 2009.
14. R. Mével, S. Javoy, and G. Dupré. A chemical kinetic study of the oxidation of silane by nitrous oxide, nitric oxide and oxygen. *Proceedings of The Combustion Institute*, 33:485–492, 2011.
15. J. Melguizo-Gavilanes, S. Coronel, R. Mével, and J.E. Shepherd. Dynamics of ignition of stoichiometric hydrogen-air mixtures by moving heated particles. *International Journal of Hydrogen Energy*, 2016.